Electronic Supplementary Material (ESI) for Journal of Materials Chemistry C.

Supporting Information

Highly Efficient Non-doped Thermally Activated Delayed Fluorescent Organic Light-emitting Diodes Using an Intra- and Intermolecular Exciplex System with a Meta-linked Acridine-Triazine Conjugate

Seongjin Jeong, Youngnam Lee, Joon Ki Kim, Du-Jeon Jang and Jong-In Hong*

Table of Contents

1. General methods

1.1 Quantum Chemical Calculations: All quantum chemical calculations were performed using the Gaussian ’09 program package. Gas-phase geometry optimizations for the lowest excited singlet and triplet states were carried out using time-dependent density functional theory calculations at the B3LYP/6-31G(d) level.

1.2 Photophysical measurements: UV-visible spectra were recorded on a Beckman DU650 spectrophotometer. Fluorescence spectra were recorded on a Jasco FP-6500 spectrophotometer. Fluorescent quantum yields in solid films were recorded on an Otsuka electronics QE-2000 spectrophotometer. Photoluminescence decay kinetic profiles were obtained by monitoring emission from a sample excited at 266 nm pulses having a duration time of 6 ns from a Q-switched Quantel Brilliant Nd:YAG laser. Photoluminescence was wavelength-selected using a Kratos GM 200 double monochromator of 0.2 m, detected using a Hamamatsu R928 PMT, and digitized using a Lecroy Wavepro 950 oscilloscope of 1 GHz. Low-temperature measurements were conducted using a cryostat (Iwatani Industrial Gases, CRT-006-2000) with application of an InGa alloy as an adhesive to ensure good thermal conductivity between the silicon substrate and the sample holder.

1.3 Electrochemical measurements: Cyclic voltammetry (CV) experiments were conducted in CH_2Cl_2 solutions (1.00 mM) with 0.1 M tetra-n-butylammonium hexafluorophosphate ($TBAPF_6$) as the supporting electrolyte. A glassy carbon electrode was employed as the working electrode and referenced to a Ag reference electrode. All potential values were calibrated against the ferrocene/ferrocenium (Fc/Fc+) redox couple. The onset potential was determined from the intersection of two tangents drawn at the rising and background current of the cyclic voltammogram.

1.4 Single crystal X-ray structure analysis: Crystallographic data of AmT (CCDC 1545856) and AmmT (CCDC 1546113) are summarized in Table S1. These data can be obtained free of charge from The Cambridge Crystallographic Data Centre via www.ccdc.cam.ac.uk/data_request/cif.

2. Synthesis and characterization

Commercially available reagents and solvents were used without further purification unless otherwise noted. ^{1}H- and ^{13}C-NMR spectra were recorded using an Agilent 400 MHz Varian spectrometer in $CDCl_3$. ^{1}H-NMR chemical shifts in $CDCl_3$ were referenced to $CHCl_3$ (7.27 ppm). ^{13}C-NMR chemical shifts in $CDCl_3$ were reported relative to $CHCl_3$ (77.23 ppm). Elemental analyses were carried out using the Flash 2000 Elemental Analyzer (Thermo Fisher Scientific, Germany).

2.1. Synthesis of 9,9-dimethyl-9,10-dihydroacridine (1, Ac). 1 was prepared according to the literature procedure.[1] Compound **1** (3.80 g, 70%) was obtained as yellowish powder. ^{1}H NMR (400 MHz, $CDCl_3$, δ): 7.37 (dd, *J* = 7.7, 1.3 Hz, 2H), 7.09 (ddd, *J* = 7.7, 7.4, 1.3 Hz, 2H), 6.91 (ddd, *J* = 7.7, 7.4, 1.3 Hz, 2H), 6.67 (dd, *J* = 7.7, 1.3 Hz, 2H), 6.10 (s, 1H), 1.57 (s, 6H); ^{13}C NMR (100 MHz, $CDCl_3$, δ): 138.6, 129.3, 16.9, 125.6, 120.7, 113.5, 36.3, 30.7.

2.2. Synthesis of 10-(3-iodophenyl)-9,9-dimethyl-9,10-dihydroacridine (2). 9,9-Dimethyl-9,10-dihydroacridine (**1**) (3.80 g, 18.15 mmol), 1,3-diiodobenzene (17.97 g, 54.47 mmol), Cu powder (0.77 g, 12.11 mmol), and potassium carbonate (10.03 g, 72.63 mmol) were introduced into nitrogen atmosphere. The mixture was heated at reflux temperature under nitrogen in dry 1,2-dichlorobenzene (200 mL). After 2 days, the reaction mixture was concentrated in vacuo and extracted with dichloromethane. The organic layer was washed with water and brine, and dried using anhydrous sodium sulfate. The filtrate was concentrated in vacuo to give a crude mixture, which was purified by column chromatography (SiO_2, CH_2Cl_2 : hexane = 1 : 9) to afford compound **2** (3.6 g, 48.2%) as a white solid. ^{1}H NMR (400 MHz, $CDCl_3$, δ): 7.84 (dd, *J* = 7.2, 1.6 Hz, 1H), 7.70 (s, 1H), 7.44 (dd, *J* = 7.2, 1.6 Hz, 2H), 7.36~7.34 (m, 2H),

6.95 (m, 4H), 6.23 (dd, *J* = 7.8, 1.2 Hz, 2H), 1.67 (s, 6H); ^{13}C NMR (100 MHz, $CDCl_3$, δ): 142.5, 140.5, 140.4, 137.4, 132.2, 131.0, 130.1, 126.4, 125.3, 120.9, 114.0, 95.3, 35.9, 31.3.

2.3. Synthesis of (3-(9,9-dimethylacridin-10(*9H*)-yl)phenyl)boronic acid (3). 10-(3-Iodophenyl)-9,9-dimethyl-9,10-dihydroacridine (**2**) was dissolved in dry THF (100 mL) under a nitrogen atmosphere. This solution was cooled to -78 ℃ followed by dropwise addition of 2.5 M n-butyl lithium solution in hexane (4.38 mL, 10.94 mmol). This mixture was stirred for 1 hour after which trimethylborate (1.57 mL, 16.41 mmol) was added. After stirring at room temperature for 15 hours, the reaction mixture was added to an aqueous solution of HCl (1 N) and stirred for 2 hours. The aqueous phase was separated and extracted with dichloromethane (3 × 50 mL). The combined organic extracts were dried using sodium sulfate, concentrated in vacuo and purified by column chromatography (SiO_2, dichloromethane : methanol = 20 : 1) to afford compound **3** (1.20 g, 66.8%) as a yellow sticky liquid. ^{1}H NMR (400 MHz, $CDCl_3$, δ): 8.10 (s, 1H), 7.91 (d, *J* = 7.2 Hz, 1H), 7.70 (s, 1H), 7.65 (t, *J* = 7.6 Hz, 1H), 7.35 (d, *J* = 8 Hz, 2H), 6.95~6.89 (m, 4H), 6.21 (d, *J* = 7.2 Hz, 2H), 5.19 (br s, 2H), 1.68 (s, 6H); ^{13}C NMR (100 MHz, $CDCl_3$, δ): 140.9, 138.4, 134.2, 133.5, 130.5, 129.9, 126.4, 126.3, 125.3, 125.2, 120.5, 114.0, 35.9, 30.1.

2.4. Synthesis of 2-(3-bromophenyl)-4,6-diphenyl-1,3,5-triazine (4). Aluminum trichloride (6.1 g, 45.57 mmol) was dissolved in 100 mL 1,2-dichlorobenzene. Thionylchloride (1.10 mL, 1.81 g, 13.67 mmol), 3-bromobenzoylchloride (6.01 mL, 10 g, 45.57 mmol), and benzonitrile (9.8 mL, 95.03 mmol) were added to the resulting solution. The mixture was stirred for 20 hours at 100 ℃. After cooling to room temperature, ammonium chloride (4.9 g, 91.61 mmol) was added to the reaction mixture and stirred for 3 hours at 100 ℃. After cooling to room temperature, the reaction mixture was poured into 350 mL methanol and stirred for 1 hour. The solid product was filtered and washed with hot ethanol. After drying under reduced pressure at 60 ℃, compound **4** (7.1 g, 40%) was obtained as a white solid. ^{1}H NMR (500 MHz, $CDCl_3$, δ): 7.37 (t, *J* = 8.0 Hz, 1H), 7.51~7.59 (m, 6H), 7.67 (d, *J* = 8.0 Hz, 1H), 8.61 (d, *J* = 8.0

Hz, 1H), 8.68 (d, *J* = 7.1 Hz, 2H), 8.80 (s, 1H); ^{13}C NMR (125 MHz, $CDCl_3$, δ): 122.8, 127.4, 128.6, 128.9, 130.0, 131.7, 32.6, 135.2, 135.8, 138.2, 170.2, 171.6.

2.5. Synthesis of 9,9-dimethyl-10-phenyl-9,10-dihydroacridine (PhAc). To a solution of 9,9-dimethyl-9,10-dihydroacridine (**1**) (0.30 g, 1.43 mmol) in dry toluene (5 mL) was added potassium carbonate (0.59 g, 4.30 mmol) and bromobenzene (0.25 g, 1.58 mmol). The reaction mixture was purged with nitrogen for 30 min, and then palladium (II) acetate (32 mg, 0.14 mmol) and tri-tert-butylphosphine tetrafluoroborate (50 mg, 0.172 mmol) were added. The reaction mixture was stirred at 110 ℃ for 12 hours under nitrogen. After being concentrated in vacuo, the reaction mixture was diluted with dichloromethane and water, extracted with dichloromethane. The organic layer was washed with water and brine solution and dried using anhydrous sodium sulfate. The filtrate was concentrated in vacuo to give a crude mixture, which was purified by column chromatography on silica gel eluted with hexane only to afford **PhAc** (0.24 g, 80.0%) as a white solid. ^{1}H NMR (300 MHz, $CDCl_3$, δ): 7.66~7.61 (m, 2H), 7.53 (d, *J* = 6.9 Hz, 1H), 7.47 (d, *J* = 7.5 Hz, 2H), 7.35 (d, *J* = 7.5 Hz, 2H), 7.00~6.92 (m, 4H), 6.26 (d, *J* = 7.8 Hz, 2H), 1.70 (s, 6H); ^{13}C NMR (75 MHz, $CDCl_3$, δ): 141.2, 141.0, 131.4, 130.9, 130.0, 128.2, 126.4, 125.2, 120.5, 114.0, 36.0, 31.3.

2.6. Synthesis of 2,4,6-Triphenyl-1,3,5-triazine (TRZ). Benzonitrile (1.00 g, 9.72 mmol) was added to trifluoromethanesulfonic acid (4.95 g, 32.96 mmol) cooled to 0 ℃ in an ice-bath and stirred for 30 min. The mixture was further stirred at room temperature overnight. Water (50 mL) was added, and the resulting mixture was neutralized with sodium hydroxide. Then, a mixture of chloroform and acetone (1 : 1 (v/v), 50 mL) was added. The organic layer was separated and the aqueous layer was extracted with a 1:2 mixture of chloroform and acetone. The combined organic layers were washed with brine, dried over magnesium sulfate, and concentrated in vacuo. 2,4,6-Triphenyl-1,3,5-triazine (0.80 g, 80.0%) was obtained as a white solid. ^{1}H NMR(300 MHz, $CDCl_3$, δ): 7.58 (m, 9H), 8.77 (d, 6H); ^{13}C NMR(75 MHz, $CDCl_3$, δ): 128.6, 129.0, 132.5, 136.2, 171.6.

2.7. Synthesis of 10-(3-(4,6-diphenyl-1,3,5-triazin-2-yl)phenyl)-9,9-dimethyl-9,10-dihydroacridine (AmT). 9,9-Dimethyl-9,10-dihydroacridine (**1**) (1.50 g, 7.42 mmol), 2-(3-bromophenyl)-4,6-diphenyl-1,3,5-triazine (**4**) (3.46 g, 8.90 mmol), palladium acetate (0.12 g, 0.52 mmol), tri-tert-butylphosphine tetrafluoroborate (0.43 g, 1.48 mmol) and potassium *tert*-butoxide (1.66 g, 14.83 mmol) were introduced into a dried 250 mL two-neck round bottom flask under an atmosphere of nitrogen. Dry toluene (70 mL) was added and heated to reflux under nitrogen atmosphere for 12 hours. The reaction mixture was concentrated in vacuo and extracted with dichloromethane. The organic layer was washed with water and brine and dried using anhydrous sodium sulfate. The filtrate was concentrated in vacuo to give a crude mixture, which was purified by column chromatography (SiO_2, hexane) to afford **AmT** (2.23 g, 58.2%) as a yellow solid. ^{1}H NMR (400 MHz, $CDCl_3$, δ): 8.95 (ddd, *J* = 8, 1.4, 1.4 Hz, 1H), 8.79~8.74 (m, 5H), 7.85 (t, *J* = 8 Hz, 1H), 7.87~7.50 (m, 9H), 6.97 (qd, *J* = 5.6, 1.2 Hz, 4H), 6.36 (dd, *J* = 8, 1.6 Hz, 2H), 1.76 (s, 6H); ^{13}C NMR (100 MHz, $CDCl_3$, δ): 171.8, 170.9, 141.7, 140.8, 139.4, 136.0, 135.6, 132.7, 132.1, 131.4, 130.0, 129.0, 129.0, 128.9, 128.7, 126.5, 125.4, 120.7, 114.1, 31.5; HRMS (ESI) *m*/*z* [EI +]: calcd for $C_{36}H_{28}N_4$, 516.2314; found, 516.2311; Elem. Anal. calcd for $C_{36}H_{28}N_4$: N 10.84, C 83.69, H 5.46; found: N 10.93, C 83.22, H 5.44.

2.8. Synthesis of 10-(3'-(4,6-diphenyl-1,3,5-triazin-2-yl)-[1,1'-biphenyl]-3-yl)-9,9-dimethyl-9,10-dihydroacridine (AmmT). (3-(9,9-Dimethylacridin-10(9H)-yl)phenyl)boronic acid (**3**) (1.60 g, 4.86 mmol), 2-(3-bromophenyl)-4,6-diphenyl-1,3,5-triazine (**4**) (1.89 g, 4.86 mmol), tetrakis(triphenylphosphine)palladium (0.28 g, 0.24 mmol) and aqueous sodium carbonate (2 M, 5 mL) in toluene (60 mL) and ethanol (5 mL) were heated to reflux in a nitrogen atmosphere for 24 h. After the reaction mixture was concentrated in vacuo, the resulting mixture was extracted with dichloromethane. The organic layer was washed with water and brine, and dried using anhydrous sodium sulfate. The filtrate was concentrated in vacuo to give a crude mixture, which was purified by column chromatography (SiO_2, ethyl acetate : hexane = 1 : 25) to afford **AmmT** (1.6 g, 55.6%) as a white solid. ^{1}H NMR (400 MHz,

$CDCl_3$, δ) δ (ppm) 9.03 (s, 1H), 8.78~8.76 (m, 5H), 7.91 (d, *J* = 7.6 Hz, 1H), 7.85 (d, *J* = 7.2 Hz, 1H), 7.78 (t, *J* = 8 Hz, 1H), 7.73 (s, 1H), 7.66~7.54 (m, 7H), 7.48 (dd, *J* = 7.6, 1.2 Hz, 2H), 7.39 (d, *J* = 8 Hz, 1H), 6.98 (m, 4H), 6.43 (dd, *J* = 7.6, 1.2 Hz, 2H), 1.72 (s, 6H); ^{13}C NMR (100 MHz, $CDCl_3$, δ): 171.7, 143.7, 141.8, 140.9, 140.6, 136.9, 136.1, 135.1, 132.6, 131.4, 131.1, 130.4, 130.1, 130.1, 129.3, 129.0, 128.7, 128.3, 127.5, 127.0, 126.4, 125.2, 120.6, 114.1, 31.1; HRMS (ESI) *m*/*z* [EI +]: calcd for $C_{42}H_{32}N_4$, 529.2627; found, 592.2628; Elem. Anal. calcd for $C_{42}H_{32}N_4$: N 9.45, C 85.11, H 5.44; found: N 9.48, C 84.89, H 5.53.

3. Supplementary tables and Figures.

Table S1. Summary of crystal structures of AmT and AmmT.

	AmT (CCDC **1545856**)	**AmmT** (CCDC **1546113**)
Empirical formula	$C_{36}H_{28}N_4$	$C_{42}H_{32}N_4$
Formula weight	516.62	592.71
Temperature (K)	295.9(8)	295.9(2)
Wavelength (Å)		
Crystal system	Orthorhombic	Orthorhombic
Space group	Pbca	Pbca
a (Å)	13.7631(7)	17.1361(10)
b (Å)	11.4154(9)	8.1119(7)
c (Å)	34.944(4)	45.473(5)
α (°)	90	90
β (°)	90	90
γ (°)	90	90
Volume ($Å^3$)	5490.0(8)	6321.0(9)
Z	8	8
Density (calculated) (g/cm^3)	1.250	1.234
Absorption coefficient (mm^{-1})	0.575	0.568
F(000)	2176.0	2496.0
Reflections collected	15633	39350
Independent reflections	5703 [R(int) = 0.0285]	6598 [R(int) = 0.0946]
2Θ range for data collection (°)	5.058 to 153.236	5.16 to 157.4
Goodness-of-fit on F^2	0.991	0.983
Final R indices [I>2sigma(I)]	R1 = 0.0438, wR2 = 0.1115	R1 = 0.0819, wR2 = 0.1981
R indices (all data)	R1 = 0.0693, wR2 = 0.1280	R1 = 0.1585, wR2 = 0.2641
Largest diff. peak and hole ($e.Å^{-3}$)	0.12 and -0.18	0.24 and -0.24

Table S2. Summary of transient PL decay data of neat and doped films of AmT and AmmT at 300 K under nitrogen.

Conditions/ Compounds	τ_1 (μs)	τ_2 (μs)	A_1[a)]	A_2[a)]		
Neat film of AmT	0.093	5.804	2.606	0.092	0.312	0.688
Doped film of AmT[d)]	0.079	4.322	3.024	0.132	0.294	0.706
Neat film of AmmT	0.059	1.761	3.328	0.372	0.229	0.771
Doped film of AmmT[d)]	0.072	4.013	0.921	0.061	0.212	0.788

[a)] A_i is the pre-exponential for lifetime; [b)] R_{PF} is the ratio of the prompt component, $R_{PF} = \tau_1A_1/(\tau_1A_1 + \tau_2A_2)$; [c)] R_{DF} is the ratio of the delayed component, $R_{DF} = \tau_2A_2/(\tau_1A_1 + \tau_2A_2)$; [d)] 20 wt% doped in DPEPO host.

Table S3. Device performances based on AmT and AmmT.

Device condition	V_{on}[a)] [V]	EQE_{max}[b)] [%]	C. $E._{max}$[c)] [cd A^{-1}]	P. $E._{max}$[d)] [lm W^{-1}]	λ_{max} [nm]	CIE (x, y)
Doped AmT[e)]	5.8	4.19	9.02	3.83	500	(0.24, 0.39)
Doped AmmT[e)]	4.1	3.28	5.67	2.97	476	(0.18, 0.27)
Non-doped AmT	3.4	5.68	15.04	5.76	524	(0.33, 0.54)
Non-doped AmmT	3.6	18.66	45.13	37.31	504	(0.24, 0.49)

[a)] Turn-on voltage at 1 cd m^{-2}; [b)] maximum external quantum efficiency; [c)] maximum current efficiency; [d)] maximum power efficiency; [e)] 20 wt% doped in DPEPO.

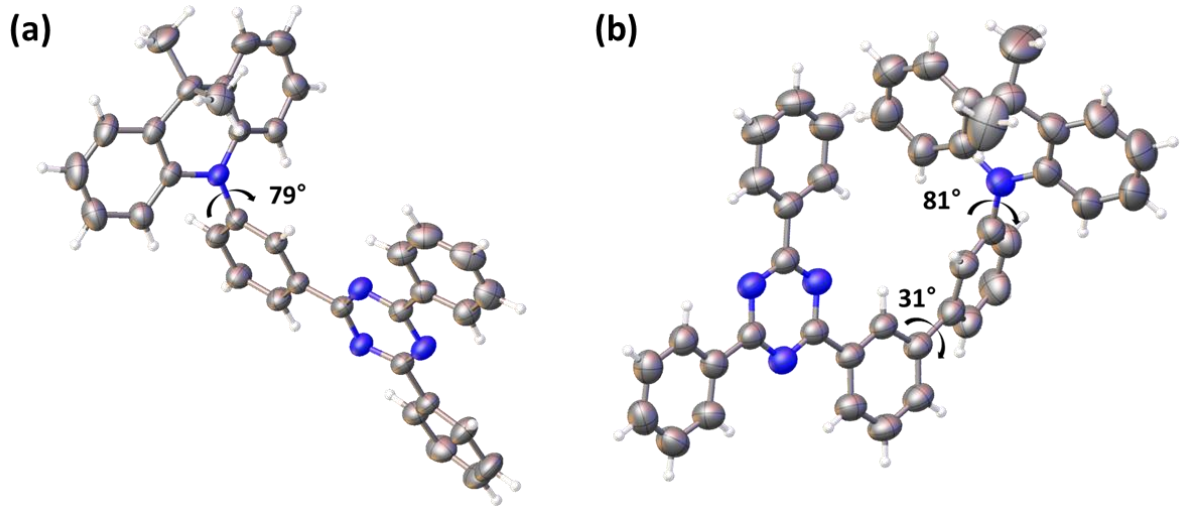

Figure S1. Single crystal structures of AmT (left, CCDC 1545856) and AmmT (right 1546113).

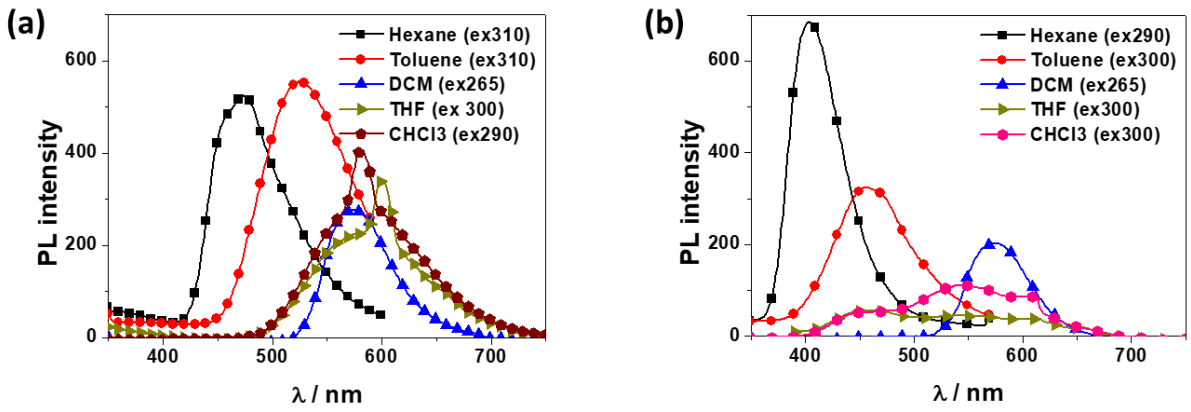

Figure S2. PL spectra of (a) AmT and (b) AmmT in various solvents (10^{-5} M).

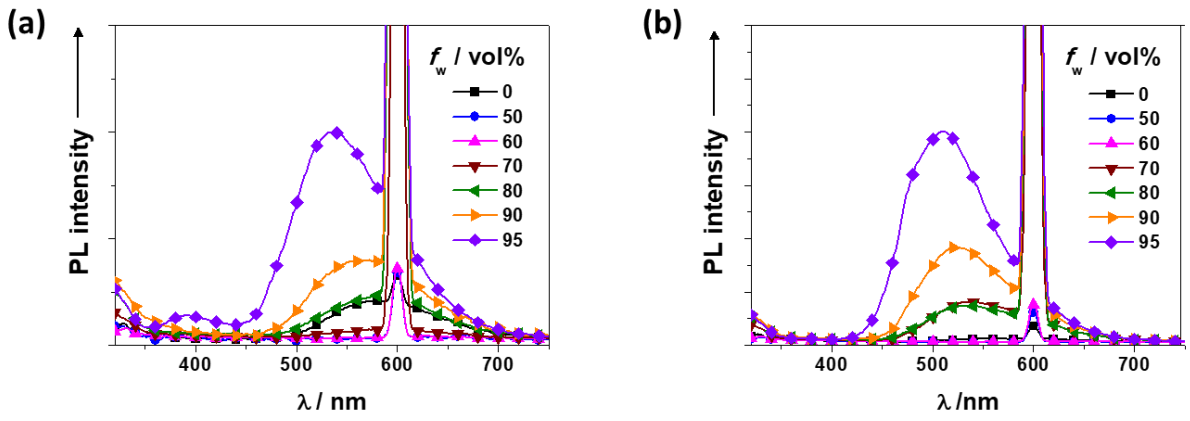

Figure S3. PL spectra in THF/water mixtures with different water fractions (f_w) of (a) AmT (b) AmmT. PL peak at 600 nm is the 2nd harmonic wavelength of excitation.

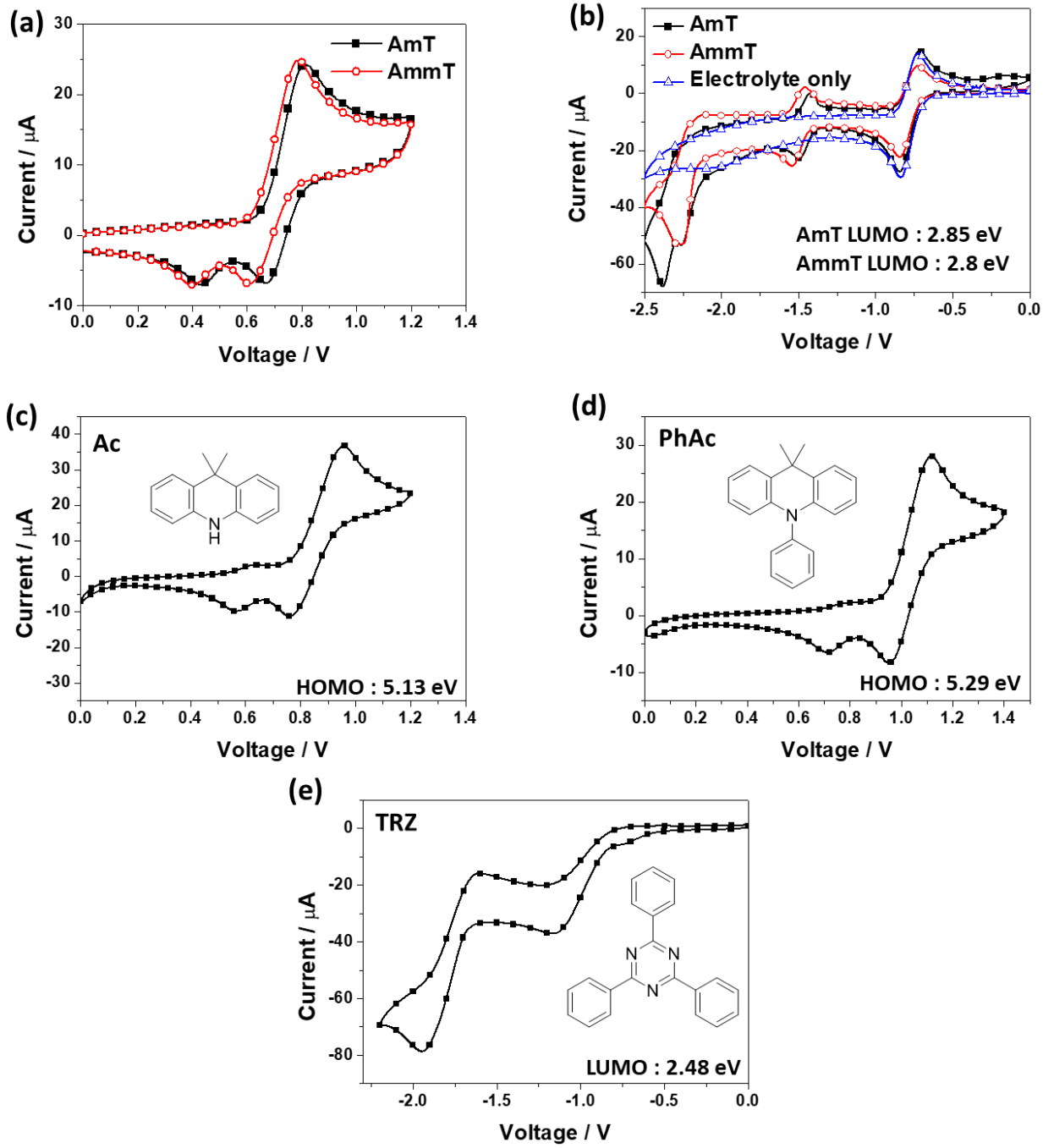

Figure S4. Cyclic voltammograms of (a), (b) AmT and AmmT, (c) Ac, (d) PhAc and (e) TRZ. The HOMO energy levels were measured by CV anodic scan in dichloromethane, while the LUMO energy levels were measured by CV cathodic scan in dimethylformamide.[2]

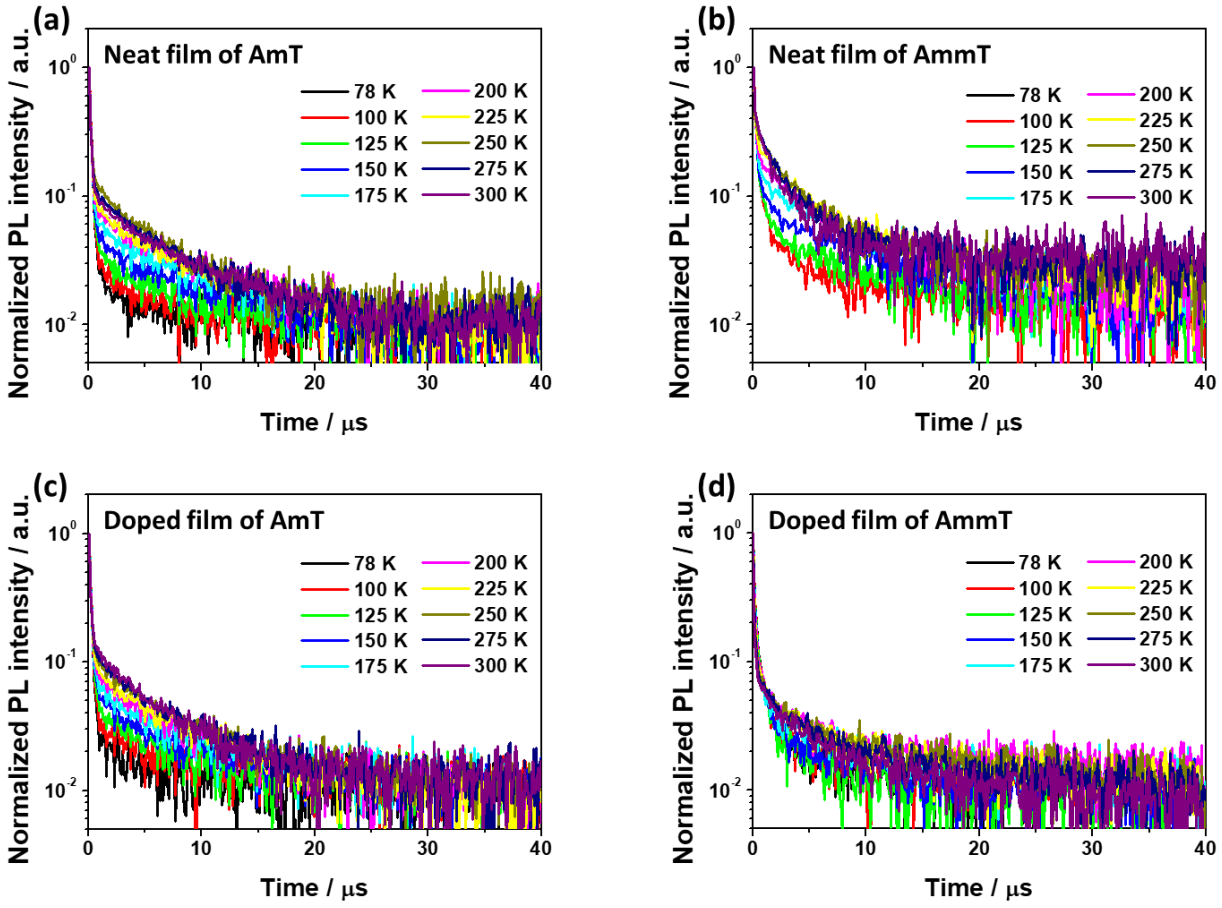

Figure S5. Temperature-dependent transient decay spectra of neat and doped films (20 wt% in DPEPO) of AmT and AmmT.

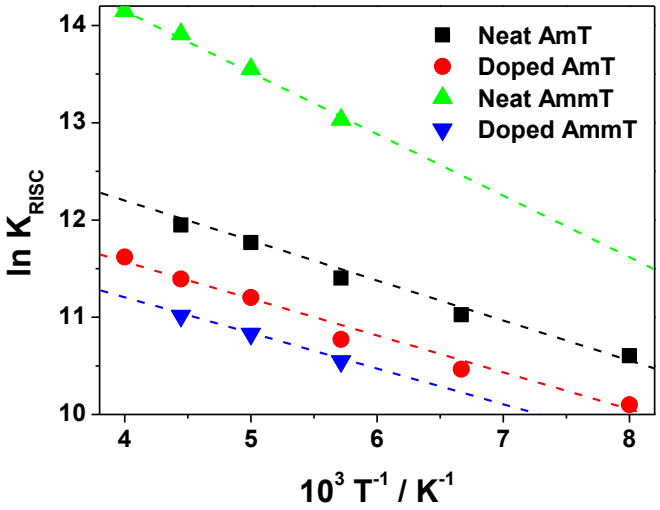

Figure S6. Arrhenius plots of the reverse ISC rate from the triplet to the singlet state of AmT and AmmT in neat and doped (20 wt% in DPEPO) films.

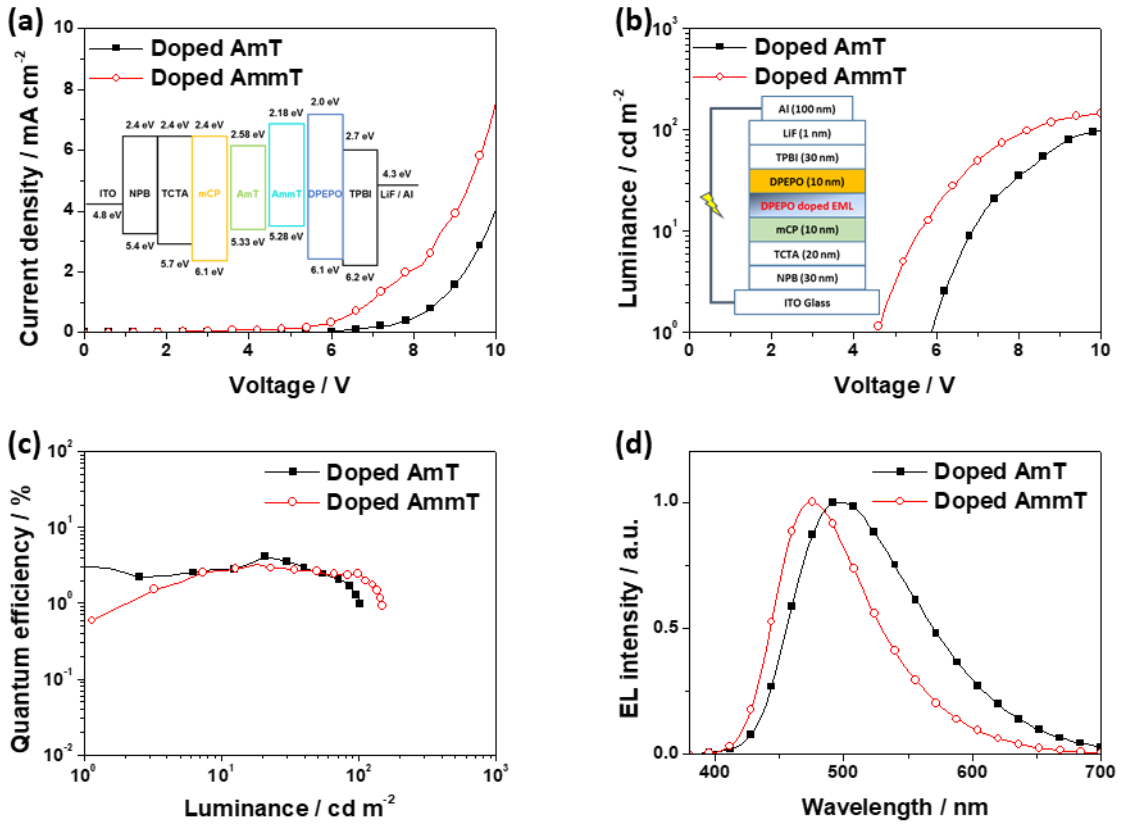

Figure S7. EL characteristics of devices fabricated using 20 wt% AmT and AmmT doped into DPEPO in the EML. (a) Current density-voltage characteristics (inset: energy level diagram of each device), (b) luminance-voltage characteristics (inset: device structure), (c) quantum efficiency-luminance characteristics, and (d) EL spectra.

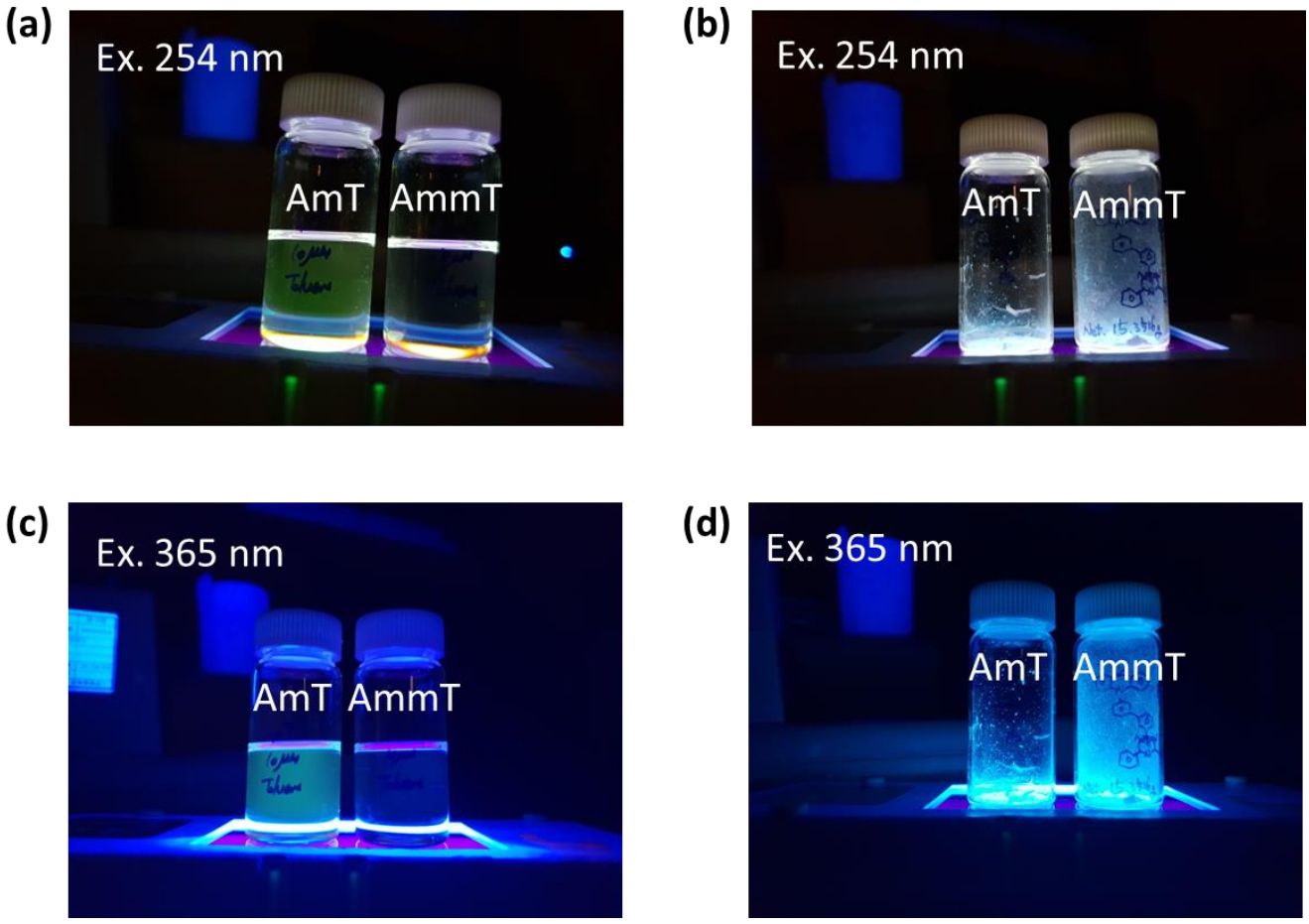

Figure S8. Emission characteristics upon excitation using UV hand lamp at 254 nm of (a) (left) 10 μM AmT and (right) 10 μM AmmT in toluene, (b) (left) AmT and (right) AmmT powder; at 365 nm of (c) (left) 10 μM AmT and (right) 10 μM AmmT in toluene, (d) (left) AmT and (right) AmmT powder.

4. Supplementary notes[3,4]

The PL quantum efficiency of prompt fluorescence (Φ_{PF}) is expressed by

$$k_{PF} = k_r^S + k_{nr}^S + k_{ISC} \quad (1)$$

$$k_{DF} = k_{nr}^T + \left(1 - \frac{k_{ISC}}{k_r^S + k_{nr}^S + k_{ISC}}\right) k_{RISC} \quad (2)$$

$$\emptyset_{PF} = \frac{k_r^S}{k_r^S + k_{nr}^S + k_{ISC}} = \frac{k_r^S}{k_{PF}} \quad (3)$$

$$\emptyset_{DF} = \sum_{n=1}^{\infty} (\emptyset_{ISC}\emptyset_{RISC})^n \, \emptyset_{PF} \quad (4)$$

$$\emptyset_{ISC} = \frac{k_{ISC}}{k_r^S + k_{nr}^S + k_{ISC}} \quad (5)$$

By assuming (i) $k_{RISC} >> k_r^T$, k_{nr}^T and Φ_{RISC} is almost 1, solving equations (1) ~ (5)

$$k_{ISC} = \frac{\emptyset_{DF} k_{PF}}{\emptyset_{PF} + \emptyset_{DF}} \quad (6)$$

$$k_{RISC} = \frac{k_{PF} k_{DF}}{k_{ISC}} \frac{\emptyset_{DF}}{\emptyset_{PF}} \quad (7)$$

k_{ISC} and k_{RISC} were estimated from equations (6) and (7)

5. References

1 S. N. Bagriantsev, K. H. Ang, A. Gallardo-Godoy, K. A. Clark, M. R. Arkin, A. R. Renslo, D. L. Minor, *ACS Chem. Biol.*, 2013, **8**, 1841-1851.
2 M. L. Pegis, J. A. S. Roberts, D. J. Wasylenko, E. A. Mader, A. M. Appel, J. M. Mayer, *Inorg. Chem.*, 2015, **54**, 11883-11888.
3 K. Goushi, K. Yoshida, K. Sato, C. Adachi, *Nat. Photonics*, 2012, **6**, 253-258.
4 J. Lee, N. Aizawa, M. Numata, C. Adachi, T. Yasuda, *Adv. Mater.*, 2017, **29**, 1604856.